The formation of hydroxyapatite–calcium polyacrylate composites

K. E. WATSON, K. S. TENHUISEN, P. W. BROWN*
Penn State University, 136 Intercollege Materials Research Laboratory, University Park, PA 16802, USA

Tetracalcium phosphate (TetCP, $Ca_4(PO_4)_2O$) reacts rapidly with polyacrylic acid (PAA). Complete reaction results in the formation of hydroxyapatite (HAp) and calcium polyacrylate. Consequently, this combination of reactants can react to form a dental cement. However, reaction occurs so rapidly that it would be difficult to achieve a homogeneous mixture of reactants suitable for use in restorations. In order to explore extending the working time, the effects of prehydrating the TetCP to form surface layers of HAp on the TetCP particles was explored. Prehydration was found to be an effective means of allowing workability. Therefore, the effects of the proportions of TetCP and PAA, with and without HAp filler, on cement properties were investigated. The extents of the reactions were investigated by X-ray diffraction analysis; the extents of PAA neutralization were studied by Fourier transform infra-red spectroscopy (FTIR); pore structures were determined by mercury intrusion porosimetry; microstructures were observed by scanning microscopy, and compressive strengths were determined. After curing for 17 days at room temperature PAA neutralization was almost complete; however, residual TetCP could be detected by X-ray diffraction and PAA by FTIR. As expected, the compressive strengths of the cements showed a dependence on the liquid (water + polymer)-to-solid (TetCP + HAp filler) used. The presence of HAp filler caused a significant decrease in compressive strength and increasing the proportion of HAp filler resulted in a decrease in the compressive strength. The characteristics of the load–deflection curves showed a dependence on the presence of HAp filler. In the absence of filler, two slopes were observed in the curves whereas a linear curve, typical of a ceramic, was observed when HAp filler was present. Mercury intrusion porosimetry (MIP) indicated the majority of the porosity was present in pores larger than 0.1 μm. Porosity increased with increasing liquid-to-solids ratio and with an increasing proportion of HAp filler at a constant liquid-to-solids ratio. Microstructural observations indicated the effect of HAp filler on increasing porosity was the result of porosity present in the filler itself. Thus, poorly consolidated HAp filler contributed to increased porosity and reduced compressive strength.

1. Introduction

Biocompatibility, tooth bonding, and durability are important attributes of dental cements. Cements that allow minimal marginal leakage to reduce the entry of caries-causing bacteria into the restoration and that support prolonged retention of restorations are highly desirable. These attributes, along with good wetting and bonding to enamel and dentine and low toxicity, have stimulated the development of new ionomer-based cements. Calcium phosphate–calcium polycarboxylate (CP–CPC) cements could prove to be very useful in this regard for several reasons. Tooth mineral is comprised of hydroxyapatite (HAp), suggesting CP–CPC to be an extremely compatible biocomposite. As the cement cures, there is a possibility of incorporating available calcium ions from the exposed tooth surface into the polymeric crosslinks, thereby eliminating a clear division between the natural tooth surface and the restoration. Such divisions tend to be problematic as time passes, frequently allowing caries-causing bacteria to get under the restoration and destroy the underlying tissue. Like glass ionomer cements (GICs), sources of leachable fluoride compounds can be mixed with CP–CPC cements to produce a cariostatic effect in the surrounding enamel [1, 2]. A few experiments using mixtures of tetracalcium phosphate ($Ca_4(PO_4)_2O$ or TetCP) and polyacrylic acid (PAA) as bone cements have shown there is no adverse tissue reaction, the cement bonds both chemically and mechanically to bone, and osteogenesis can and will occur in areas adjacent to the cement restorations [3, 4]. These findings suggest that TetCP-PAA cements might be a potentially superior material for use in dental technology as well as for the fixation of prostheses to bone.

*To whom correspondence and reprint requests should be addressed.

It is possible to produce hydroxyapatite–calcium polyacrylate cements [5] by reactions similar to those of glass-ionomer or zinc polycarboxylate (ZP) cements [6]. It has been demonstrated [7, 8, 9] that the hydrolysis of calcium phosphate mixtures containing TetCP by inorganic or organic acids produce calcium polyacrylate and hydroxyapatite which, in a similar form, comprises much of the natural tooth structure. The reaction is very similar to that of GIC cements, but in this case the product is a calcium polyacrylate instead of a calcium aluminum polyacrylate. The formation of HAp as one of the products of the reaction results in a cement that is more biocompatible than ZPs or GICs. Particulate TetCP (Ca/P = 2) converts in aqueous solution to HAp (Ca/P $\sim$ 1.67) with the extra calcium ions neutralizing the carboxyl sites on the PAA. However, it is difficult to constitute a usable cement by this reaction. Reaction is so rapid, the setting rate precludes working the material.

Interest in producing a cement that is more like the tooth itself has stimulated research to find a means to control the rate of the TetCP–PAA reaction. One method of controlling the reaction rate is addition of other polymers or copolymers to the acid solution. Several studies have used organic acids such as citric acid [10] and tartaric acid [1, 2] as an additive. Citric and tartaric acids are useful because they both increase working time and give a sharp set by complexing available metal ions [11]. Other acids used include malic acid [12, 13], acrylic–itaconic acid copolymers, and acrylic–fumaric acid copolymers [14]. The reaction has also been retarded using other additives, such as tribasic sodium phosphate and metal fluorides [8]. Finally, a method of controlling the reaction by partially hydrating TetCP was studied [14]. Such partial hydration forms apatite-coated TetCP particles, which react with PAA at a much slower rate than do uncoated particles.

The strengths of these cements have been shown to be on the same order as those of ZP cements. For example, TetCP cements produced using citric acid and/or tartaric acid [2, 15] have been shown to exhibit compressive strengths in the range of 64–88 MPa. The TetCP cement that had the highest strength reported used a 40% PAA solution and attained a compressive strength of 150 MPa [16]. Another study using a PAA-itaconic acid copolymer solution produced a cement with a tensile strength of 12.37 MPa, which is much higher than reported for most currently available cements [17, 18].

Many factors have been shown to have an effect on strength. As the powder-to-liquid ratio increases, compressive strength increases up to a maximum value, which varies from material to material. Most cements reach strength maxima when the powder-to-liquid ratio is in the range of 1.3-to-1 to 2-to-1 [11, 19]. At higher ratios, the mechanical properties of the cement begin to decrease as the powder begins to interfere with the crosslinking of the polymer in solution. It has also been shown that changes in the calcium-to-phosphate ratio have an affect on compressive strength. As shown in one study, when the calcium-to-phosphate ratio of one citric acid cement changes from 1.8-to-1 to 2-to-1, compressive strength decreases from 88 MPa to 64 MPa [15]. Some of the additives used to control the reaction rate of the cement will also change mechanical properties. It has been shown [8] that increasing the concentration of tribasic sodium phosphate or metal fluorides added to a PAA cement reduces the mechanical properties. However, it was also found that with 8% stannous fluoride and 10% tartaric acid added, mechanical properties and setting were much improved.

The mechanical properties of TetCP-PAA cements also change with time. A linear increase in compressive strength as a function of time has been observed [20]. It has also been shown that after about a year, there is about a 10% increase in compressive strengths of PAA cements [21] with the average values increasing from about 60 MPa at 283 days to about 65 MPa at 472 days. It has been postulated that this is due to a corresponding increase in ionic crosslinks [22].

The present study is based on previous work [14] showing that hydration of TetCP particles will produce a coating of HAp on the surface of the particles. This is a very useful development because the HAp reacts slowly with an acidic polyelectrolyte in solution and must dissolve off the TetCP particles before the rate of reaction will accelerate; thus, the working time is increased. The aim of this study was to determine the extent of TetCP hydration needed to produce an adequate working time but still allow the occurrence of the cement-forming reaction. After this had been achieved, the effects of the inorganic-to-organic ratio and the liquid-to-solids ratio on cement properties were determined.

2. Materials and methods

2.1. Synthesis of precursors

TetCP was prepared by high-temperature reaction of reagent grade monetite ($CaHPO_4$ or calcium hydrogen phosphate, Fisher Scientific, Fair Lawn, NJ) and calcium carbonate (precipitated calcium carbonate, Fisher Scientific, Fair Lawn, NJ). These were mixed at a Ca/PO_4 ratio of 2 and fired for 2 h at 1400 °C. A sample of the product was analyzed by X-ray diffraction and found to be phase pure TetCP; CaO, which would be indicative of incomplete reaction, was not observed. HAp synthesis was very similar to that of TetCP, but the Ca/PO_4 ratio used was 1.67. This mixture was fired for 24 h at 1125 °C. X-ray diffraction patterns of the compounds formed are shown in Fig. 1. A small proportion of whitlockite ($\beta - Ca_3(PO_4)_2$) was present in the HAp formed. However, the reactivity of this phase is very low and its presence would not have a significant effect on the TetCP-PAA reaction. The TetCP was hand ground to 30 mesh and then mechanically milled to a median size of 3.0 μm. The HAp filler material was ground to pass through a 125 μm sieve.

2.2. TetCP hydration

TetCP hydration was carried out at 25 °C by stirring the TetCP particles in deionized water at a water-to-TetCP weight ratio of 5-to-1. Initially hydration was allowed to proceed for 16.5 h after which the material was dried at 200 °C for another 16.5 h. It was assumed this amount of hydration would very thoroughly coat the TetCP particles with HAp and would slow the reaction dramatically. By trial and error it was determined that 14 h was an optimal

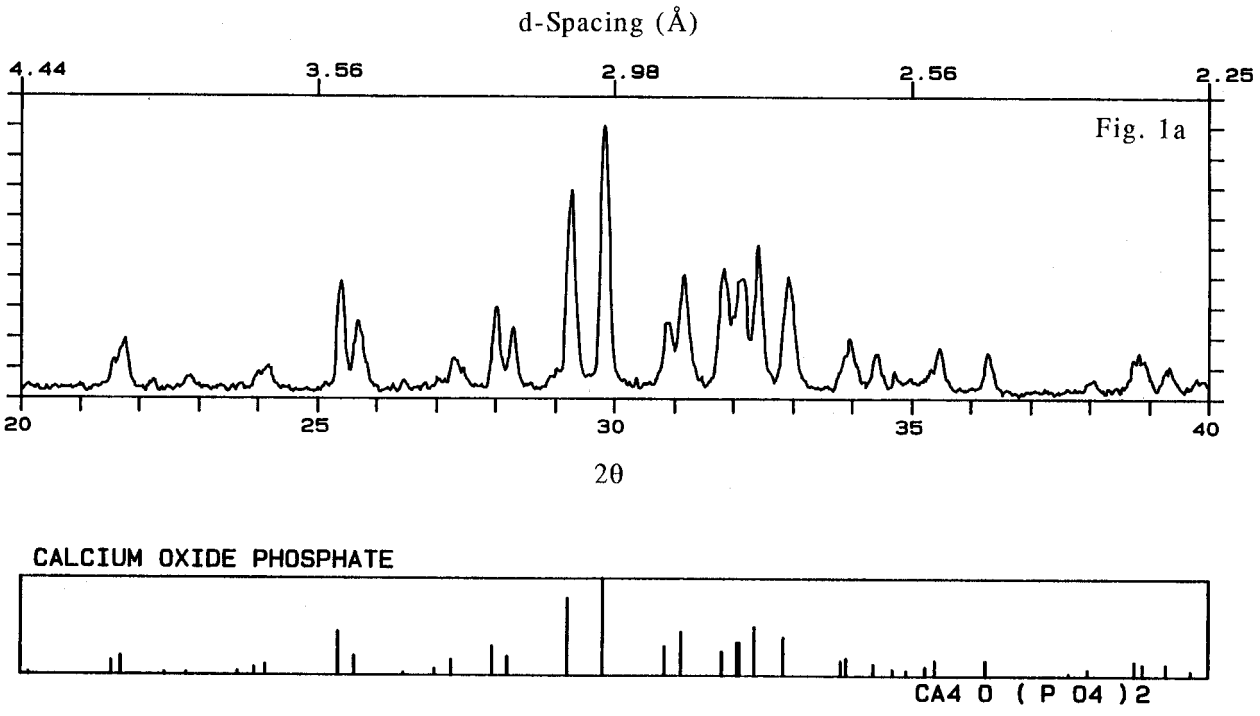

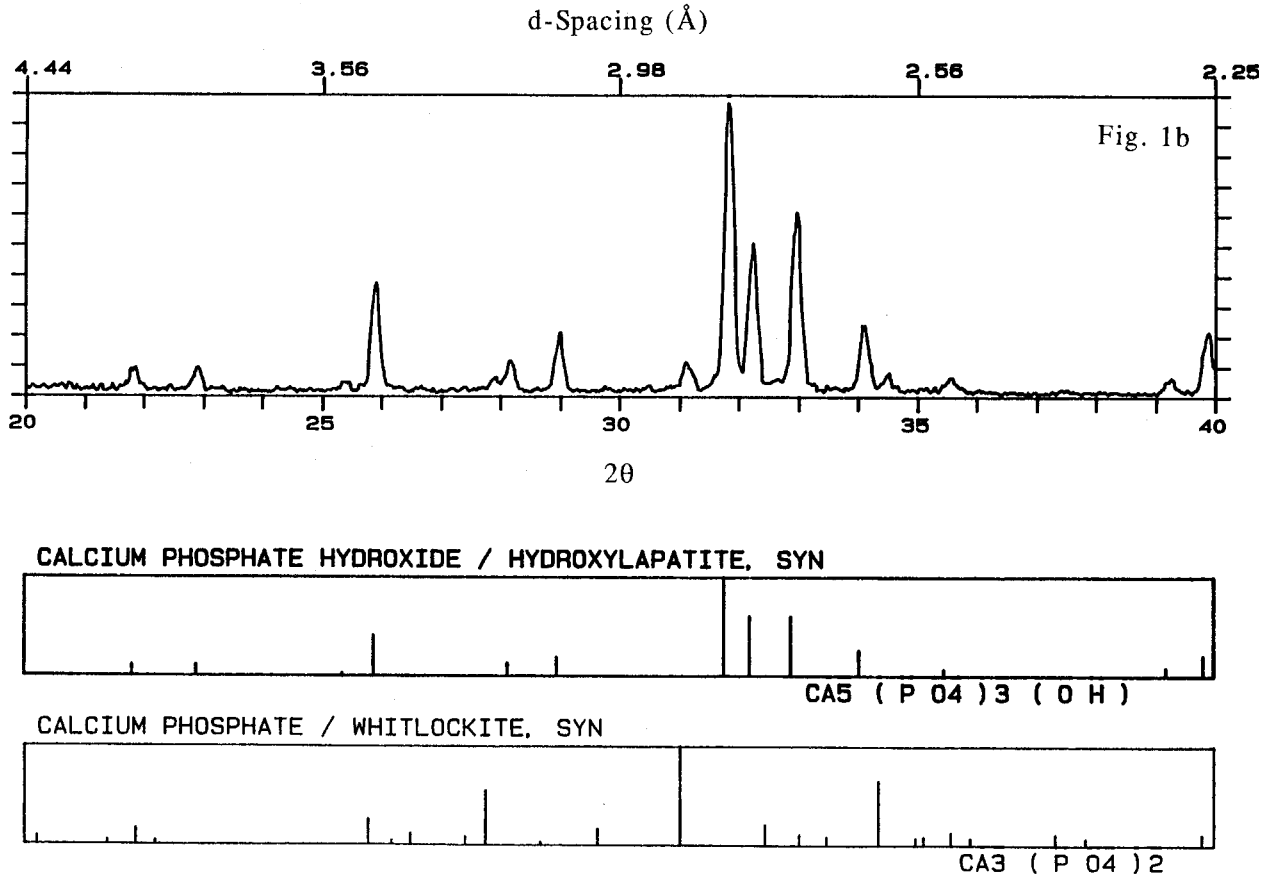

Figure 1 X-ray diffraction patterns of the reactants used in this study. (a) The diffraction pattern for TetCP. The absence of CaO peaks is indicative of phase-pure TetCP. (b) The diffraction pattern for the HAp filler, minor β-tricalcium phosphate peaks can be observed.

length of TetCP hydration for the particle sizes used. Prehydration for this length of time delayed setting for a long enough period to allow the mixtures to be placed into the molds.

2.3. Composite preparation

A 25 wt % PAA (average molecular weight by viscometry = 50 000) solution (Polysciences, Inc., Warrington, PA) was used. If water was required to adjust the liquid-to-solid ratio, it was added to the PAA solution. The TetCP-to-polymer weight ratio was held at a constant value of 3-to-1 in all of the experiments. Powder-to-polymer ratios greater than 3-to-1 were achieved by adding HAp filler. If HAp filler was used, it was mixed with the TetCP prior to composite formation [23]. The solid and liquid components were initially mixed for 30 s by hand. After hand mixing, the material was subjected to 1 min of high shear mechanical mixing. The homogenized mixtures were transferred via a specially fitted syringe into 50 mm segments of glass tubing with an inner diameter of 10 mm. These were then centrifuged at 3000 r.p.m. for about 1.5 min to minimize entrapped air, sealed with waxed plastic caps and placed in a constant temperature bath to cure at 37 °C. Table I lists the weight ratios of constituents studied. Liquid refers to the polymer solution throughout this study.

The samples were allowed to cure for 17 days. This length of time was selected to allow the reactions to approach completion. After curing, the samples were cut into 20 mm long cylinders using a diamond saw and removed from the glass cylinders. The samples were subsequently stored in a moist environment to prevent dehydration until their strengths were determined.

2.4. Composite characterization

2.4.1. Compressive strength testing

The moist 10 × 20 mm cylinders were tested (ATS 1101 mechanical testing machine, Applied Testing Systems, Butler, PA) to determine their ultimate compressive strengths and their stress–strain characteristics. A cross-head speed of 0.75 mm min^{-1} was used.

2.4.2. X-ray diffraction (XRD) analysis

Phase identification was performed using an automated powder diffractometer (Scintag Inc., Sunnyvale, CA) interfaced with a microVAX computer. The X-ray source was CuK_α radiation. Inorganic samples were ground dry with a mortar and pestle and packed into recessed glass slides; cement samples were ground in acetone with a mortar and pestle, dried, and then packed into recessed glass slides. All samples were scanned from 20–40° at a rate of 2° 2θ per minute using a step size of 0.02°.

TABLE I Initial cement compositions

Sample number	Powder-to-polymer (weight ratio)	Liquid-to-solids (weight ratio)
1	3-to-1	0.8-to-1
2	3-to-1	1.3-to-1
3	5-to-1	0.8-to-1
4	5-to-1	1-to-1
5	7-to-1	0.8-to-1
6	7-to-1	1-to-1

2.4.3. Fourier transform infrared (FTIR) spectroscopy

All cements were analyzed using FTIR spectroscopy (Perkin-Elmer, Model 1600) to determine the extent of PAA neutralization. Freeze-dried samples were stored in an evacuated desiccator containing Drierite. The samples were ground with spectroscopic grade KBr (Aldrich Chemical, Milwaukee, WI) using a mortar and pestle at a sample : KBr weight ratio of 1 : 100. Pellets were pressed and immediately analyzed. All spectra were collected at a resolution of 4 cm^{-1} and 265 scans were made for each sample over a range of 500–4500 cm^{-1}.

2.4.4. Mercury intrusion porosimetry (MIP)

Samples were prepared for MIP analysis by crushing to sand-sized grains and then freeze-drying to ensure removal of all water. Analysis was carried out using a scanning mercury intrusion porosimeter (model 9300, Quantachrome Corp., Syosset, NY) and data was collected on an IBM PC using MIP data collection software. Pressure versus volume data were transferred to a graphing program and plotted as pressure versus % volume (intruded volume/total sample volume).

2.4.5. Scanning electron microscopy

Microstructures of the fracture surfaces of the samples were observed using an environmental scanning electron microscope (SEM, ElectroScan, Wilmington, MA). Typical magnifications used were 1000 × and 5000 ×.

3. Results

3.1. Compressive strength determinations

Composite samples were tested wet in order to more closely simulate composite conditions *in vivo*. The lower limit on the liquid-to-solids ratio was 0.8-to-1; at ratios lower than this a significant reduction in workability was observed. Values of the peak loads obtained in the testing of compressive strength are presented in Table II. The sample sets used are small ($N = 2$ to $N = 4$) and the results obtained were intended to establish the effects of the liquid-to-solids and powder-to-polymer weight ratios on the strength. Fig. 2 shows load-deflection curves typical of sample set 1 and sample set 5 (from Table II).

3.2. FTIR spectra

FTIR spectra were obtained using specimens retrieved from the compressive strength measurements. These were carried out to determine the extent of PAA neutralization. Fig. 3 is typical of the specta obtained.

TABLE II Compressive strength data

Sample number	Powder-to-polymer (weight ratio)	Liquid-to-solids (weight ratio)	Peak load (MPa)
1.1	3-to-1	0.8-to-1	25.02
1.2	3-to-1	0.8-to-1	22.22
2.1	3-to-1	1.3-to-1	11.21
2.2	3-to-1	1.3-to-1	11.40
3.1	5-to-1	0.8-to-1	14.11
3.2	5-to-1	0.8-to-1	13.72
3.3	5-to-1	0.8-to-1	14.02
3.4	5-to-1	0.8-to-1	13.19
4.1	5-to-1	1-to-1	14.14
4.2	5-to-1	1-to-1	15.01
4.3	5-to-1	1-to-1	14.87
4.4	5-to-1	1-to-1	13.80
5.1	7-to-1	0.8-to-1	15.88
5.2	7-to-1	0.8-to-1	16.56
5.3	7-to-1	0.8-to-1	17.48
5.4	7-to-1	0.8-to-1	15.52
6.1	7-to-1	1-to-1	13.40
6.2	7-to-1	1-to-1	12.81
6.3	7-to-1	1-to-1	15.14

3.3. Mercury intrusion porosimetry

MIP data are presented in Fig. 4. Sample 1 contained far less water than any of the other samples, and was expected to exhibit far lower porosity (in agreement with compressive strength tests).

3.4. X-Ray diffraction analysis

Fig. 5 shows the diffraction patterns representative of sample sets 1 and 5. Both patterns show HAp diffraction peaks. The presence of a small proportion of unreacted TetCP is indicated by the labeled peaks.

3.5. Environmental scanning electron microscopy (ESEM)

Figs 6 and 7 show ESEM micrographs of fracture surfaces obtained from compression testing of sample set 1 and sample set 6, respectively. Examination of the filler by conventional scanning electron microscopy (see Fig. 8) revealed that larger, coarse particles of the filler (about 50 μm) were actually partially sintered masses of much smaller particles (< 3 μm).

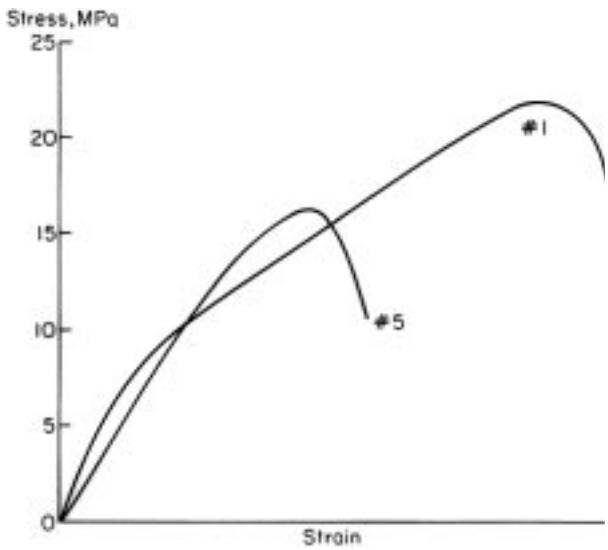

Figure 2 Load–deflection curves representative of those observed. The curve from sample set 1 is typical of those obtained in the absence of HAp filler while the curve from sample set 5 was typically observed when HAp filler was present.

4. Discussion

As would be expected, the compressive strengths show a dependence on the liquid-to-solids ratio. Increasing the liquid-to-solids ratio in the absence of HAp filler from 0.8 to 1.3, results in a reduction of strength by a factor of about 2 (see Table II). This results from an increase in the porosity with a change in the liquid-to-solids ratio as shown in Fig. 4. Comparing sample sets 1, 3, and 5 (Table II), where the liquid-to-solids ratio is constant (0.8) and the proportion of HAp filler increases, shows that the addition of HAp filler reduced the compressive strength of these composites when compared to sample set 1. Sample sets 4 and 6, which also contain varying amounts of HAp filler at a constant liquid-to-solids ratio of 1, showed a decrease in compressive strength with respect to sample set 1. The compressive strengths of these composites appeared to be influenced primarily by the presence or absence of HAp filler, with the relative proportion of the filler causing a smaller effect. All samples containing HAp filler exhibited similar compressive strengths regardless of its proportion or the liquid-to-solids ratio.

The character of the load-deflection curves also changed depending on the presence or absence of HAp filler. The curve from sample set 1 (Fig. 2) is typical of composites containing no HAp filler and is characterized by two regions. At low loads there was a region typical of the behavior of ceramics where the slope of the curve is both linear and steep. At about 30% of the peak load a slope change occurred and a second linear region is observed. This is a result of the presence of the polymer. The presence of HAp filler in these composites resulted in one nominally linear slope as shown in Fig. 2 for sample set 5. This suggests the stress–strain relationship was predominantly affected by high temperature HAp-PAA interaction. The slope of the curves in the samples containing HAp filler (sample sets 3–6) are intermediate between the two slopes observed in the curves of sample set 1.

Trends in porosity, as determined by MIP, corresponded to changes in both the relative amount of filler at constant liquid-to-solids ratio and to changes in the liquid-to-solids ratio at constant powder-to-polymer ratios. Such variablity is in accord with the results obtained when PAA-ZnO cements were studied [24]. At a liquid-to-solids ratio of 1, the porosity increased as the proportion of HAp filler increased (i.e. as the powder-to-polymer ratio increased). This is shown by comparing samples 1, 3, and 5. This must be a result of the porosity present in the HAp filler particles which will subsequently be discussed. The porosity was significantly higher for those samples containing HAp filler as compared to samples 1 and 2. This corresponds to the lower strength values obtained for samples 3–6 as compared to sample 1. A decrease in the ultimate

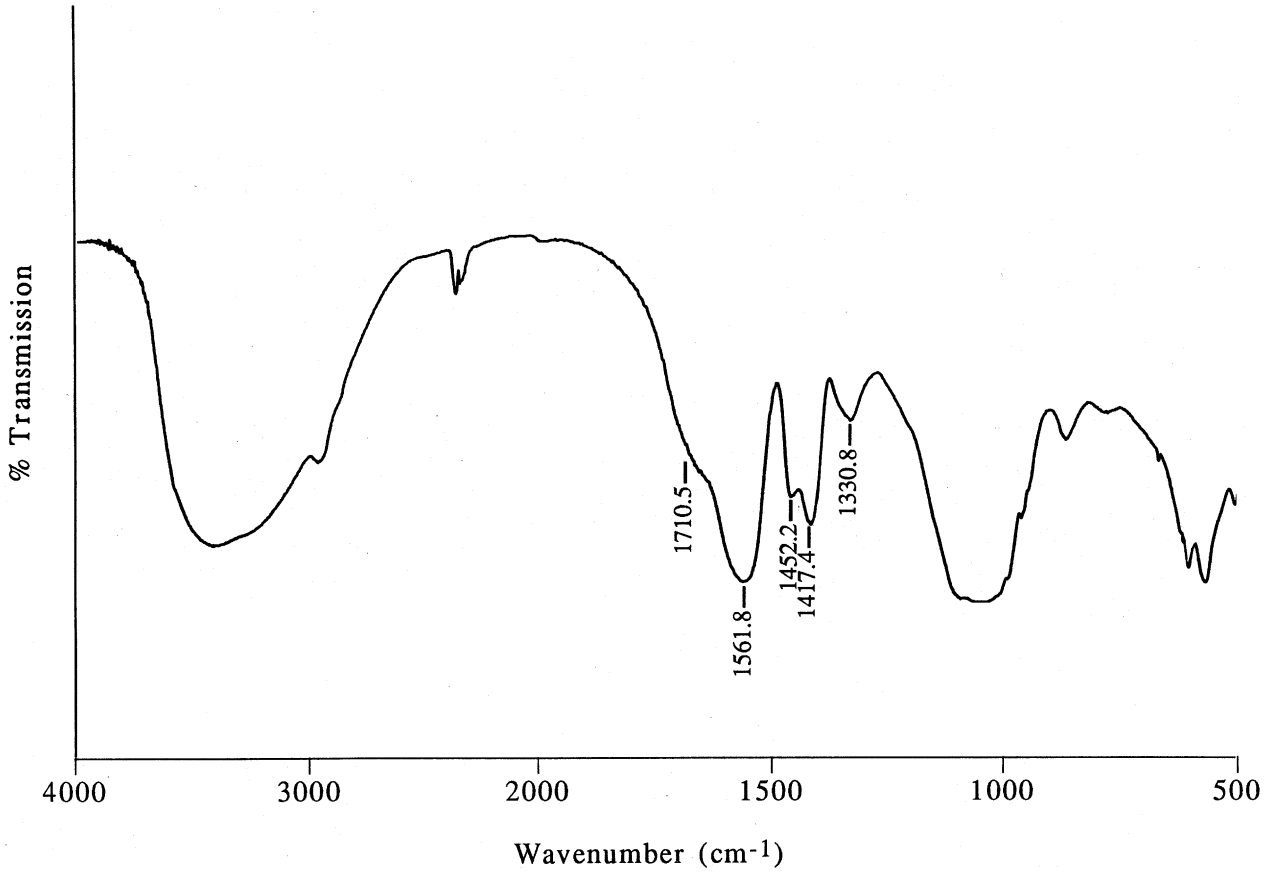

Figure 3 An FTIR spectrum typical of those obtained in this study. The spectrum is characterized by peaks indicative of the formation of calcium polyacrylate (1562, 1415–1417, 1330 cm^{-1}) along with a small proportion of unneutralized polymer (1730 cm^{-1}).

strength would be expected as porosity was introduced into a material.

Comparing samples 1 and 2 shows the porosity increased as the liquid-to-solids ratio increased at constant powder-to-polymer ratios. This should occur since water results in residual porosity. Again, a decrease in the compressive strength was observed as the porosity increased under these conditions. Anomalous to these predictable trends was the compressive strength of sample 2 compared to those of samples 3–6. Based on porosity, sample 2 should have a higher compressive strength than samples 3–6. This was not the case. As shown in Table II, sample 2 exhibited the lowest compressive strength observed in this study. This result presently cannot be explained. Both samples 1 and 2 showed similar degrees of reaction with respect to TetCP and PAA. The above findings suggest the compressive strength was highly sensitive to both the polymer and water content. The presence of HAp filler appeared to be detrimental to the mechanical properties. This was likely caused by the microstructure of the filler material. It would appear that using higher polymer content composites and minimizing the amount of water is required to optimize the mechanical properties in the present system.

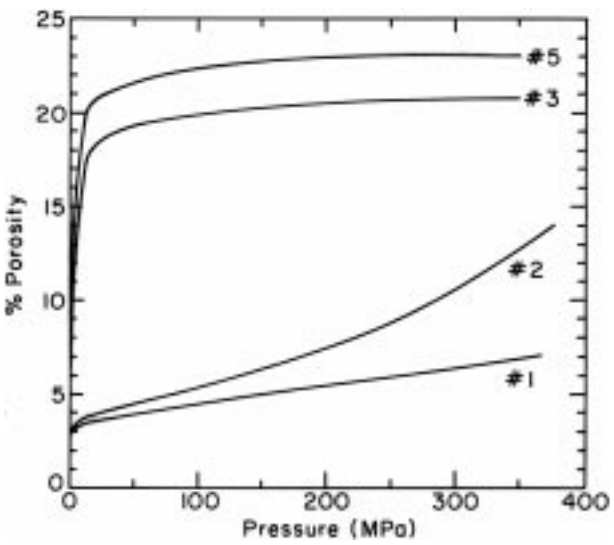

Figure 4 Plot showing the porosity, as determined by mercury intrusion porosimetry, in a variety of composites depending on the intrusion pressure.

As indicated by the MIP data, the majority of the porosity is greater than 0.1 μm. This is evident by the sharp increase in porosity intruded at low applied pressures (< 10 MPa). This is also evident in the microstructure. It should be noted there was a small proportion of small pores as apparent by the slight increase in porosity over the intrusion pressure range of $\sim$ 10–350 MPa. These small pores were likely a result of the HAp formed from reactions between TetCP and PAA. These reactions have been shown to produce extremely small crystallites of HAp [5] which in turn can result in small pores due to the nature of the reaction. The fact that the slope of porosity versus pressure over the range of $\sim$ 10–350 MPa increases with a decrease in the powder-to-polymer ratio further supports this hypothesis.

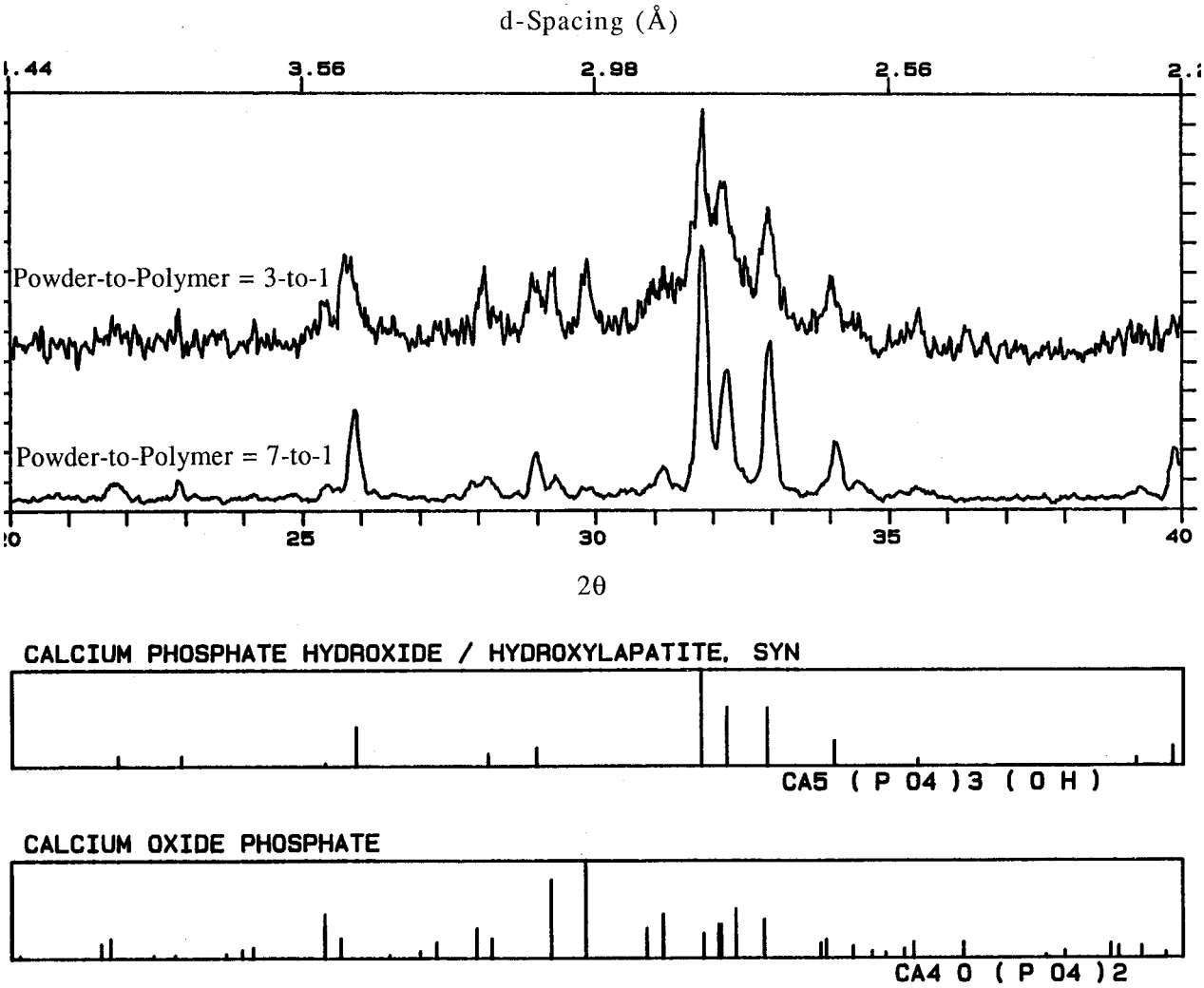

Figure 5 X-ray diffraction patterns indicating the formation of HAp and the presence of a small proportion of unreacted TetCP.

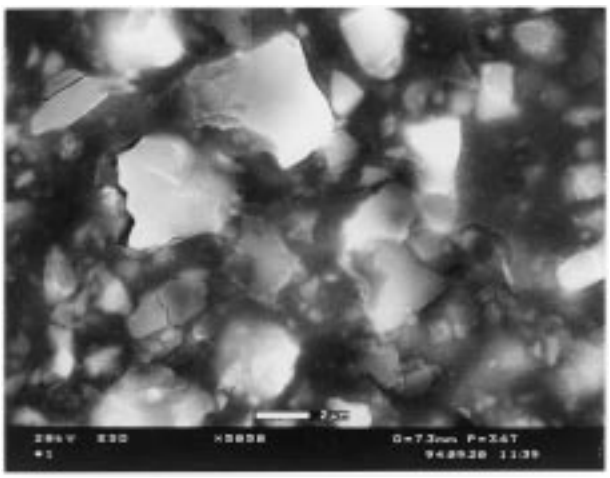

Figure 6 Micrograph showing a fracture surface of a composite that does not contain HAp filler.

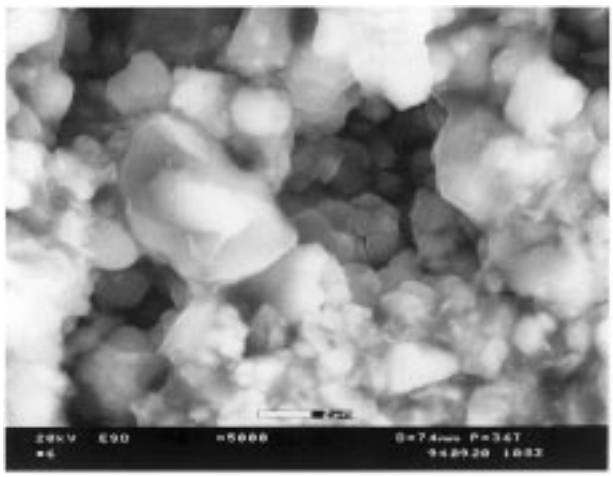

Figure 7 Micrograph showing a fracture surface of a composite containing HAp filler. Compared to the micrograph in Fig. 6, significantly more porosity is present.

Table III lists selected i.r. frequencies of PAA and its calcium salt. The strong peak at about 1562 cm^{-1} is that of neutralized polymer. The small peak at around 1330 cm^{-1} is also from neutralized polymer, as is the peak at about 1415–1417 cm^{-1}. However, the continuation of the shoulder up to about 1730 cm^{-1} is indicative of a small proportion of unneutralized polymer. While polymer neutralization was nearly complete, the presence of some unreacted acidic carboxylate groups was expected because X-ray diffraction indicates the presence of residual TetCP in all samples. The presence of residual TetCP as observed by X-ray diffraction indicates the system can exhibit the reserve alkalinity necessary to preclude the occurrence of low pH due to residual unneutralized PAA carboxyl groups.

Sample set 1 did not contain HAp filler. Thus, the HAp

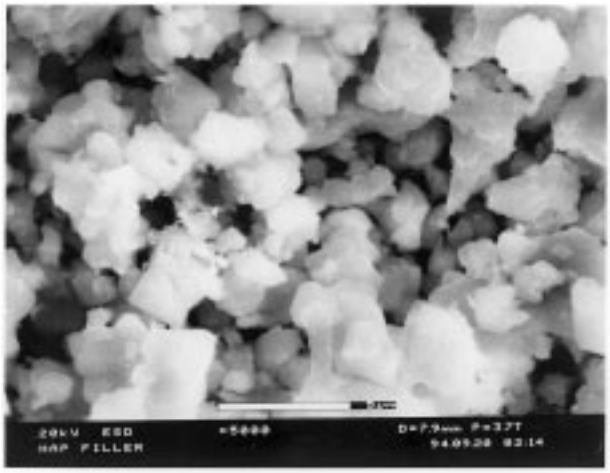

Figure 8 Microstructure of the HAp filler material showing it to be highly porous and poorly consolidated.

TABLE III Selected infrared frequencies of PAA and its calcium salt

Infrared Bands (cm^{-1})		Assignments
$\alpha = 0$ (pure acid)	$\alpha = 1$ (pure salt)	
3150 (m)		ν (OH)
1730 (sh), 1709 (s)		ν(C=O)
	1562 (s)	ν_{as}(COO)
1451 (m)	1452 (m)	$\delta(CH_2)$ (bending)
1414 (w)		ν(CO)/δ(OH) interaction
	1417 (s)	ν_s(COO)
	1320–1350 (m)	δ(CH), $\gamma_w(CH_2)$
1247 (m)		ν(CO)/δ(OH) interaction
1171 (m)		ν(COOH)

δ = deformation, ν_s = symmetric stretching, γ_w = wagging, and ν_{as} = asymmetric stretching s = strong, m = medium, and w = weak intensities; sh = shoulder

formed was the result of the reaction of TetCP with PAA. HAp formed in this way was comprised of very small crystallites. These result in X-ray diffraction patterns exhibiting broad diffraction peaks with relatively low intensities. The HAp present in sample set 6 appeared more crystalline in that the diffraction pattern was dominated by the diffraction peaks of the filler. Comparing the relative intensities of the residual TetCP peaks in the two patterns shows them to be approximately the same. This suggests the presence of the HAp filler did not significantly promote the conversion of TetCP to HAp by providing sites for epitaxial growth. The presence of small amounts of unreacted TetCP was likely a result of a CPA–HAp coating forming on the surfaces of the TetCP particles due to the reaction between PAA and the TetCP. This layer ultimately results in a diffusionally controlled reaction [5]. These data, along with those from FTIR analysis, indicate extensive TetCP/PAA reaction. This suggests that the relatively low strengths observed were principally the result of elevated porosity and not from incomplete reaction.

Figs 6 and 7 show representative microstructural features of composites prepared with and without the HAp filler. As indicated by MIP data and supported by compressive strength results, samples prepared without HAp filler (Fig. 6) showed very small amounts of porosity. The sample appears relatively homogeneous and is characterized by particles on the order of 0.5–5 μm dispersed within a polymer matrix. While X-ray diffraction showed the mineral phase was primarily HAp, the microstructure of the particulate material is reminiscent of the TetCP precursor. As mentioned previously, there was a much higher proportion of porosity observable in the samples containing the HAp filler (Fig. 7). This resulted from the internal porosity of the partially sintered HAp agglomerated filler (see Fig. 8). The filler particles did not become completely infiltrated with polymer because of the lower relative proportion of PAA in these samples. Fig. 8 shows the microstructure of one agglomerated particle. It is apparent this particle is composed of partially sintered HAp crystallites 0.5–2 μm in size. Filler HAp likely would have been more effective in these composites if the particles were dense sintered grains or large single crystals. This would have reduced the porosity of samples containing filler resulting in higher strengths.

Acknowledgment

The authors gratefully acknowledge the support of NSF DMR 9510272.

References

1. K. MIYAZAKI, T. HORIBE, J. M. ANTONUCCI, S. TAKAGI and L. C. CHOW, *Dent. Mater.* **9** (1993) 41.
2. U. SAITO, K. FUKUDA and S. UNE, Ube Industries, assignee. Japanese patent 03215406. Sept. 20, 1991.
3. Y. YOSHIMINE, A. AKAMINE, M. MUKAI, K. MAEDA, M. MATSUKURA, Y. KIMURA and T. MAKISHIMA, *Biomaat* **4** (1993) 403.
4. C. A. VAN BLITTERSWIJK, J. R. DE WIJN, H. LEENDERS, J. VAN DEN BRINK, S. C. HESSELING and D. BAKKER, *Cells Mater.* **3** (1993) 11.
5. K. TENHUISEN and P. W. BROWN, *J. Dent. Res.* **73** (1994) 598.
6. G. J. CHRISTENSEN, *JADA* **120** (1990) 59.
7. L. C. CHOW, S. TAKAGI, P. D. COSTANTINO and C. D. FRIEDMAN, *Mater. Res. Soc. Symp. Proc.* **179** (1991) 3.
8. K. MIYAZAKI, T. HORIBE, J. M. ANTONUCCI, S. TAKAGI and L. C. CHOW, *ibid.* **9** (1993) 46.
9. L. XIE and E. A. MONROE, *Mater. Res. Soc. Symp. Proc.* **179** (1991) 25.
10. Y. HIBINO and H. HASHIMOTO, *Meikai Daigaku Shigaku Zasshi* **21** (1992) 555.
11. R. G. CRAIG, W. J. O'BRIEN and J. M. POWERS, ''Dental materials: properties and manipulation,'' (Mosby Year Book, St Louis, 1992).
12. F. SUGIHARA, M. YAMADA, S. AKAMATSU, S. SHIMADA, K. TOYOOKA, I. KISHIDA, Y. MANDAI and H. OONISHI, *Seitai Zairyo* **4** (1986) 199.
13. A. IMURA and T. SAITO, Osaka Cement Co., assignee. Manufacture of tetracalcium phosphate and its hardening products. Japanese patent 02180705. July 13, 1990.
14. A. IMURA, T. SAITO and S. IKEGAMI, Osaka Cement Co., assignee. German patent 4124898. Jan. 30, 1992.
15. Y. KOTEGAWA, S. MOTOI, S. MATSUNO, S. HINAKO, TAKEHIKO, K. MORI, K. SUGAWARA, K. K. FURUTEGAWA and K. K. INTERUHATSU, Japanese patent 03040952. Feb. 21, 1992.
16. T. SHIOSU and K. K. HAIRU, assignee. Japanese patent 85-77201. Apr. 11, 1986.
17. A. SUGAWARA, J. M. ANTONUCCI, S. TAKAGI, L. C. CHOW and M. OHASI, *J. Nihon Univ. Sch. Dent.* **31** (1989) 372.

18. A. SUGAWARA, Seiwa Corporation, assignee. Japanese patent 02250810. Jan 8, 1990.
19. Y. HIBINO and H. HASHIMOTO, *Meikai Daigaku Shigaku Zasshi* **21** (1992) 566.
20. Y. FUKASE, E. D. EANES, S. TAKAGI, L. C. CHOW and W. E. BROWN, *J. Dent. Res.* **69** (1990) 1852.
21. J. L. DRUMMOND, J. W. LENKE and R. G. RANDOLPH, *Dent. Mater.* **4** (1988) 38.
22. A. D. WILSON, ''Acid-base cements'', Cambridge University Press (1993).
23. P. W. BROWN and M. FULMER, *J. Amer. Ceram. Soc.* **74** (1991) 934.
24. A. PADILLA, A. VAZQUEZ, G. VAZQUEZ-POLO, D. R. ACOSTA and A. CASTAÑO, *J. Mater. Sci.: Mat. Med.* **1** (1990) 154.

Received 30 July
and accepted 31 August 1998